Density functional theory and molecular dynamics simulation study on corrosion inhibition performance of mild steel by mercapto-quinoline Schiff base corrosion inhibitor.
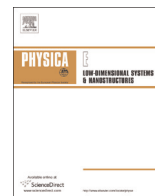
1 AUTHOR:

Sourav Saha
Central Mechanical Engineering Research I…
11 PUBLICATIONS **34** CITATIONS

SEE PROFILE

Density functional theory and molecular dynamics simulation study on corrosion inhibition performance of mild steel by mercapto-quinoline Schiff base corrosion inhibitor

Sourav Kr. Saha [a,b], Pritam Ghosh [a], Abhiram Hens [b,c], Naresh Chandra Murmu [a], Priyabrata Banerjee [a,b,*]

[a] Surface Engineering & Tribology Group, CSIR-Central Mechanical Engineering Research Institute, Mahatma Gandhi Avenue, Durgapur 713209, West Bengal, India
[b] Academy of Scientific & Innovative Research, Anusandhan Bhawan, 2 Rafi Marg, New Delhi 110001, India
[c] Micro System Technology Group, CSIR-Central Mechanical Engineering Research Institute, Mahatma Gandhi Avenue, Durgapur 713209, West Bengal, India

HIGHLIGHTS

- Performance of two mercapto-quinoline Schiff base as corrosion inhibitor was investigated theoretically.
- Quantum chemical calculations and molecular dynamics simulation were performed.
- Fukui indices have been used to analyze the local reactivity of the studied inhibitors.
- Theoretical calculations agree well with the experimental findings.

GRAPHICAL ABSTRACT

Corrosion inhibition performances of two mercapto-quinoline Schiff base inhibitors have been performed and have correlated their experimentally observed inhibition efficiency by density functional theory and molecular dynamics simulation.
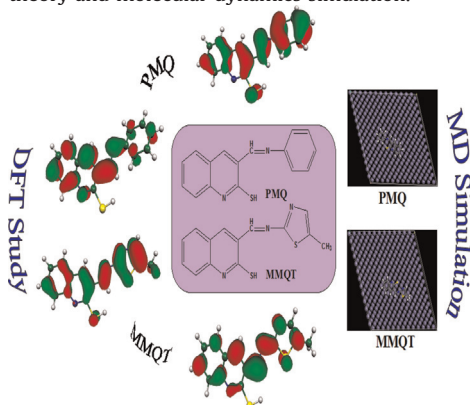
ARTICLE INFO

ABSTRACT

Corrosion inhibition mechanism of two mercapto-quinoline Schiff bases, *eg.,* 3-((phenylimino)methyl) quinoline-2-thiol (PMQ) and 3-((5-methylthiazol-2-ylimino)methyl) quinoline-2-thiol (MMQT) on mild steel surface is investigated by quantum chemical calculation and molecular dynamics simulation. Quantum chemical parameters such as E_{HOMO}, E_{LUMO}, energy gap (ΔE), dipolemoment (μ), electronegativity (χ), global hardness (η) and fraction of electron transfers from the inhibitor molecule to the metallic atom surface (ΔN) have been studied to investigate their relative corrosion inhibition performance. Parameters like local reactive sites of the present molecule have been analyzed through Fukui indices. Moreover, adsorption behavior of the inhibitor molecules on Fe (1 1 0) surface have been analyzed using molecular dynamics simulation. The binding strength of the concerned inhibitor molecules on mild steel surface follows the order MMQT > PMQ, which is in good agreement with the experimentally determined inhibition efficiencies. In view of the above, our approach will be helpful for quick

* Corresponding author at: Surface Engineering & Tribology Group, CSIR-Central Mechanical Engineering Research Institute, Mahatma Gandhi Avenue, Durgapur 713209, West Bengal, India. Fax: +91 3432546 745.
E-mail address: pr_banerjee@cmeri.res.in (P. Banerjee).

Quantum chemical calculations
Molecular dynamics simulation

prediction of a potential inhibitor from a lot of similar inhibitors and subsequently in their rational designed synthesis for corrosion inhibition application following a wet chemical synthetic route.

1. Introduction

Nowadays use of acid solutions in numerous industrial techniques such as acid pickling, acid cleaning, oil acidification, petrochemical industries, *etc.* are very common [1–3]. Those acid solutions result in serious metallic corrosion further resulting in a huge economic loss. Among several widely used methods, the most effective and economic method is to dissolve inhibitors in acid solutions to prevent the metallic corrosion [4,5]. Nature is changing in a drastic way and keeping this in mind, shielding of metal surface from corrosion is a commendable job in the field of material science. In this context, development of low cost and easy-to-make organic inhibitors is highly demanding from industrial point of view. In this field, the experimental fact obtained from several researchers have pointed out that organic compounds containing nitrogen, oxygen and sulphur-like hetero-atoms show better inhibition efficiency in different destructive media [6,7]. In general, inhibitor molecules adsorb on the metallic surface following a physical or chemical adsorption route and eventually a protective layer is formed [8–10]. Physical adsorption is regarded as electrostatic interactions between the inhibitor molecules and metallic surface whereas chemical adsorption happens by the charge sharing or transfers from the inhibitor molecules to the metallic surface [11]. The efficiency of the inhibitor molecule on metallic surfaces is directly proportional to the strength of the newly formed bonds. Inhibitors having N, O and S donor sites, unsaturated bonds along with planar conjugated aromatic moieties are preferred as good corrosion inhibitors, considering their capability to donate available lone pair of electrons or acceptance of electrons in empty low-lying d-orbital of metals [12–14]. Traditionally, weight loss, polarization curves, electrochemical impedance spectroscopy are main routes for testing inhibition performance; however, these are all high cost, time consuming microcosmic inhibition processes [15,16]. In view of the above, quantum chemical and molecular dynamics simulation is the most authentic technique which has enormous advantages of evaluating microcosmic inhibition performance and exploration of their mechanism well in advance.

Among the available computer simulation methods, determination of geometry optimized electronic structure as well as mechanism of inhibition of the so-called organic inhibitor molecules can be successfully elucidated by quantum chemical calculations [17–21]. Recently, substantiate attempt is found in the literature for the use of quantum chemical calculation as an influential theoretical tool to analyze surface-inhibitor interactions [21]. In general, frontier molecular orbital energy, fraction of electron transfer from inhibitor molecule to metallic surface, dipole moment and global hardness are considered as parameters to obtain the inhibition performance of organic inhibitor molecules in many cases [22,23]. However, Kokali et al. have proposed that only quantum chemical calculation is not sufficient enough to envisage the trend of inhibitive performance of corrosion inhibitors [24–26]. In many cases, computed outcomes obtained from quantum chemical calculations cannot be correlated with the proper experimental findings [27,28]. Therefore, a precise modeling of experiments should be emphasized for visualizing the interaction of inhibitor molecules with metal surfaces. This modeling will help to correlate the theoretical and experimental findings in an improved manner. Quantum chemistry calculations are usually accurate in terms of total electron calculation, while disadvantages are their

huge work load execution and being time-consuming too. In real practice, sometimes it is difficult to deal with any large system having hundreds or thousands of atoms. Henceforth, compared to quantum chemistry, molecular dynamics are obviously better choices keeping it in mind that only atom−atom interaction is calculated whereas in no way electron–electron interactions are considered. Molecular dynamics (MD) simulation is therefore introduced, which can provide the actual interfacial configuration and adsorption energy of the surface adsorbed inhibitor molecules [29,30]. Till date a few groups are only working on it to understand the interaction mechanism of inhibitor molecules with the metallic surface. Xia et al. recently studied the relationship between structural conformation of imidazoline derivatives and their inhibition efficiencies by applying MD simulation [31]. Yang et al. have also employed this sophisticated tool to study the adsorption behavior of thiosemicarbazone type inhibitor molecules on mild steel surface [32].

As a part of our ongoing research, we have studied both quantum chemical calculation and MD simulation to correlate the theoretical results with experimental outcomes [33,34]. The aim of this present work is to find out an alternative approach to correlate the corrosion inhibition performance of an inhibitor on a metal surface without doing any wet chemical experimentation, which obviously deserves certain importance from economic point of view. Our first and foremost duty will be to correlate the theoretical results with recently available literature reports on experimental findings. Keeping it in mind, we have executed both quantum chemical calculation and MD simulation on the recently studied selective heterocyclic inhibitor molecules, namely, 3-((phenylimino)methyl)quinoline-2-thiol (PMQ) and 3-((5-methyl-thiazol-2-ylimino)methyl)quinoline-2-thiol (MMQT) over a steel surface in acidic media [35]. The results obtained from theoretical studies are in good accordance with experimental outcomes. In this perspective, for finding out promising unexplored corrosion inhibitors, before doing hard core synthetic and wet chemical experimentation or any other expensive experimental studies we may check their efficacy as a corrosion inhibitor by simple theoretical experimentation. These findings must be helpful for rational designing of a promising corrosion inhibitor. However, till date literature survey has revealed that instances of analogous studies of a complete agreement of experimental results with theoretical outcomes are relatively less [36].

2. Computational details

2.1. Quantum chemical calculation

Geometry optimization and various quantum chemical parameters are obtained by density functional theory (DFT) calculations using the ORCA program package (ORCA is a highly flexible, efficient and easy-to-use general purpose tool for quantum chemistry; version 2.7.0) [37]. DFT is a most widely accepted ab initio approach for modeling ground states of molecules. Geometry optimizations and exchange correlations are treated using hybrid B3LYP [38–41] and full optimization is performed with SVP/SV(J) basis set, which is well accepted to provide accurate geometry and electronic properties of molecules. The all-electron Gaussian basis sets are developed by the Ahlrichs group [42]. In this calculation, triple-ζ quality basis sets TZV(P) with one set of

polarization functions on the atoms like N and S are hereby used [43]. For atoms like carbon and hydrogen, slightly smaller polarized split-valence SV(P) basis sets are used which are of double-ζ quality in the valence region and have a polarizing set of d functions on the nonhydrogen atoms. Self consistent field (SCF) calculations are tightly converged [1×10^{-8} Eh in energy, 1×10^{-7} Eh in the density change, and 1×10^{-7} in maximum element of the direct inversion in the iterative subspace or direct inversion of the iterative subspace (DIIS) error vector]. All DFT calculations are done in the aqueous phase because it is well known that the electrochemical corrosion always appears in an aqueous medium. This method is used for modeling water as a continuum of uniform dielectric constant (ε) and the solute is placed as a uniform series of inlocking atomic spheres.

Reactive sites of the molecule have been analyzed by evaluating Fukui indices (FIs). The FI calculations are performed using Dmol^3 module, Material studio™ version 6.1 by Accelrys Inc., San Diego, CA [44]. All the calculations were performed using double numerical polarization (DNP) basis set (which includes both d and p orbital polarization functional) in combination with generalized gradient approximation (GGA) and Becke–Lee–Yang–Parr (BLYP) exchange-correlation functionals [45,46]. Detailed information of local reactivity has been obtained by condensed Fukui functions [47]. The Fukui function f_k is defined as the first derivative of the electronic density $\rho(\vec{r})$ with respect to the number of electrons N in a constant external potential $v(\vec{r})$ [48].

$$f_k = \left(\frac{\partial \rho(\vec{r})}{\partial N} \right)_{v(\vec{r})} \tag{1}$$

The Fukui functions can be written by taking the finite difference approximations as [49]

$$f_k^+ = q_k(N+1) - q_k(N) \text{ (for nucleophilic attack)} \tag{2}$$

$$f_k^- = q_k(N) - q_k(N-1) \text{ (for electrophilic attack)} \tag{3}$$

where q_k is the gross charge of k atom, *i.e.;* the electronic density at a point r in space around the molecule. The q_k ($N+1$), $q_k(N)$ and q_k ($N-1$) are defined as the charge of the anionic, neutral and cationic species, respectively. Here Fukui functions are presented through the finite difference approximation using Hirshfeld population analysis (HPA) [50].

2.2. Molecular dynamics simulation

MD simulation is a technique which is popular towards exploratory studies of interaction between inhibitor and the concerned metal surfaces. The interaction between inhibitors and iron (Fe) surface is investigated by MD simulation using Material Studio™ software 6.1 (from Accelrys Inc.) [44]. Herein, we have chosen Fe (1 1 0) surface for simulation. Among other optional Fe surfaces [*e.g.*; Fe (1 0 0), Fe (1 1 1) *etc.*], Fe (1 1 0) surface is picked up for its packed surface and better stabilization. The interaction between Fe (1 1 0) surface and inhibitor molecules is carried out in a simulation box ($32.27 \times 32.27 \times 70.26$ Å) with periodic boundary conditions. A vacuum slab of 50 Å height is kept over the Fe (1 1 0) surface. The number of layers is chosen in a way that the depth of the surface is greater than the non-bonded cut-off radius used in this calculation. Thirteen layers of Fe atoms provide sufficient depth to overcome the issues related to the cut-off radius in this case. During the simulation process all the bulk Fe atoms in the Fe (1 1 0) surface are kept frozen, only inhibitors are allowed to interact with the metal surface freely. The interaction of inhibitors on the Fe (1 1 0) surface is then simulated by condensed phase optimized molecular potentials for atomistic simulation studies

(COMPASS) force field. COMPASS is the most authentic ab initio force field that ensures the accurate and simultaneous prediction of chemical properties for a wide range of chemical entities. In general, the parameterization procedure can be divided into two phases: ab initio parameterization and empirical optimization [51]. The MD simulation is performed at 298.0 K under canonical ensemble (NVT) using a time step of 1.0 fs and a simulation time of 50 ps.

The interaction energy as well as binding energy between the inhibitor molecules and Fe (1 1 0) surface is calculated using Eqs. (4) and (5) [44].

$$E_{\text{interaction}} = E_{\text{total}} - (E_{\text{surface}} + E_{\text{inhibitor}}) \tag{4}$$

$$E_{\text{binding}} = - E_{\text{interaction}} \tag{5}$$

where E_{total} is the total energy of the surface and adsorbed inhibitor molecule, E_{surface} is the energy of the surface without the inhibitor and $E_{\text{inhibitor}}$ is the energy of the adsorbed inhibitor molecule on the surface. The binding energy of the inhibitor molecule is the negative value of the interaction energy [52]. Solvent and charge effects are ignored in simulations and all calculations are performed at the metal/vacuum interface.

3. Results and discussion

3.1. Quantum chemical calculations

3.1.1. Equilibrium geometry structure

The bond lengths (Å) and bond angles (°) of the optimized neutral PMQ and MMQT molecules are calculated at the B3LYP level of theory in aqueous phase and the values are presented in Table 1. It is observed (*vide* Table 1) that the C–N bond lengths in the quinoline rings of both the molecules are longer than the general C–N double bond length (1.280 Å) and shorter than the general C–N single bond (1.470 Å) [53]. The average in bond length is an indication of conjugation in the pyridine unit of the quinoline ring. This conjugation effect in turn restricts the free rotation of C–N bonds in the pyridine rings, thereby resulting in a rigid planar structure of the corresponding quinoline ring. In PMQ (Fig.1a), one of the benzene rings is connected with the quinoline ring *via* simple azomethine group and it can be concluded (*vide* Table 1) that all the C–C bond lengths are lying in the range of (1.380–1.443) Å, which clearly shows the presence of a conjugation effect. Similarly for MMQT (Fig.1b), 5-methylthiazole unit is also connected with the quinoline segment by the azomethine linkage. It is evident from Table 1 that all the C–C, C–N and C–S bonds are in the range of 1.373 Å, 1.310–1.369 Å, 1.748–1.786 Å, which are shorter than the single bond lengths and greater than the double bond lengths [54]. The tendency of average bond in the bond length indicates a conjugation effects in the thiazole ring.

From Table 1, it could be seen that all the bond angles of quinoline and benzene rings in PMQ molecule lie in the range of 116.30–123.48°. These angles are closer to 120°, which means the atoms in PMQ are sp^2 hybridized. In case of MMQT, bond angles of quinoline and thiazole ring are in the range of 116.41–123.34° and 89.35–117.12° [55]. This result indicates that the atoms of MMQT are also sp^2 hybridized. From the above theoretical experimentation and successive discussion, it can be concluded that the optimized molecular structures of two mercapto-quinoline Schiff base inhibitors possessed ideal plane geometrical configuration.

3.1.2. Frontier molecular orbitals

It is well known that the reactivity of molecules depends entirely on the electronic distribution of their molecular orbitals. Frontier molecular orbitals are the controlling unit to investigate

Table 1
Bond length (Å) and bond angle (°) of the optimized neutral form of inhibitor molecules.

Geometry parameters	PMQ	MMQT
Bond length		
C3–C4	1.423970	1.424361
C3–C8	1.380861	1.380575
C4–C5	1.432276	1.432759
C5–C6	1.420823	1.420120
C6–C7	1.382664	1.382920
C7–C8	1.421150	1.421195
C4–C9	1.412760	1.411319
C9–C10	1.389541	1.391773
C10–C11	1.443119	1.444852
C11–N12	1.313834	1.312782
C11–S13	1.795735	1.794558
N12–C5	1.363673	1.364181
C14–C15	1.408875	1.373759
C14–C16	1.396643	–
C16–C17	1.401656	–
C17–C18	1.400693	–
C18–C19	1.398161	–
C19–C15	1.410171	–
C14–N18	–	1.369715
C15–S16	–	1.748056
S16–C17	–	1.786657
C17–N18	–	1.310070
Bond angle		
C3–C4–C5	119.47	119.50
C4–C5–C6	119.22	119.22
C6–C7–C8	120.39	120.93
C7–C8–C3	120.24	120.24
C4–C5–N12	121.38	121.42
C5–C4–C9	117.11	117.15
C9–C10–C11	116.30	116.41
C10–C11–N12	123.48	123.34
C14–C15–C19	119.03	–
C15–C14–C16	120.44	–
C16–C17–C18	119.58	–
C17–C18–C19	120.46	–
N18–C17–S16	–	112.94
C14–C15–S16	–	108.67
C17–N18–C14	–	111.93
C15–C14–N18	–	117.12
Torsion angle		
C1–N2–C15–C19	− 37.23	–
C1–N2–C15–C14	145.34	–
C1–N2–C17–S16	–	4.26
C1–N2–C17–N18	–	− 176.05

the molecular reactivity. HOMO is associated with the electron donating capability of the molecule, whereas LUMO is related to its capability of accepting electrons. HOMO orbital of geometry optimized inhibitor molecules (*e.g.*, PMQ and MMQT) have electron density over the entiremolecules (Fig. 2). This is generally due to the presence of conjugation effect. PMQ and MMQT can donate their electrons to vacant d-orbitals of acceptor Fe for the formation of co-ordinate type bonds. In PMQ, the LUMO electron density in the C–C region of quinoline segment molecule is higher, indicating the preferred active sites of accepting electrons are mainly located

in this region. For MMQT, LUMO electron density is not restricted in a particular region, rather it is distributed on the entire molecule (Fig.2). It is therefore reasonable to assume that only quinoline ring of PMQ is responsible for accepting electrons whereas all the parts of molecule MMQT are susceptible in accepting electrons from d-orbitals of metal by back bonding.

From the geometry optimized structure (Fig.2), it is observed that both the molecules are almost planar. However, in PMQ molecule the benzene ring is slightly inclined at an angle with respect to the main quinoline backbone. In MMQT, the thiazole ring is almost planar with respect to the quinoline ring. Therefore it is necessary to analyze the torsion angle in the nonlinear chain of atoms in the pivotal joining part. From Table 1, it could be seen that in PMQ the planes formed by the C1, N2, C15, C19 and C1, N2, C15, C14 atoms have torsion angles − 37.23 and 145.34, respectively, whereas for MMQT molecule, the torsion angles for C1, N2, C17, S16 and C1, N2, C17, N18 atoms are 4.26 and − 176.05°. From these results it can be concluded that irrespective of signs the torsion angles in MMQT molecule are close to 0–180°, whereas in PMQ molecule the torsion angles are not close to 0–180°. These deviations in torsion angles confirm about the unparallel orientation of two individual units (quinoline and benzene) connected by the azomethine linkage in PMQ molecule. Therefore, PMQ gets adsorbed in more or less tilted orientation on the metal surfaces and eventually its disposition to the metal surface is prevented. On the other hand, in case of MMQT a flat or parallel disposition on the metal surface has happened. This is one of the imperative reasons behind the lower inhibition efficiency of PMQ in comparison with MMQT.

3.1.3. Frontier orbital energies

The frontier molecular orbital energies of the two studied inhibitors obtained from quantum chemical calculations using ORCA program package (version 2.7.0) [37] are depicted in Table 2. Quantum chemical parameters, such as E_{HOMO}, E_{LUMO}, the energy gap between HOMO and LUMO orbitals (ΔE), dipolemoment (μ), electronegativity (χ), global hardness (η) and fraction of electron transferred (ΔN) are herein tabulated. Generally, it is assumed that E_{HOMO} is related to the capability of a molecule to donate electrons. Higher the E_{HOMO} value, stronger will be the ability of the molecules to donate electrons [56]. From Table 2, it can be concluded that E_{HOMO} values of the two inhibitor molecules obey the order PMQ < MMQT, which is in good agreement with the experimentally determined inhibition efficiencies [35].

The energy of LUMO (E_{LUMO}) signifies the ability of molecules to accept electrons from the metal surface. Lower the value of E_{LUMO}, greater is the ability of the molecule to accept electrons [50]. The values of E_{LUMO} (*vide* Table 2) are remarkably less in the order of MMQT > PMQ. This outcome again supports the fact that the relative inhibition efficiencies of two inhibitors are in line.

The energy gap (ΔE) between HOMO and LUMO exhibits the reactivity of the molecules towards the metal surface [57]. The reactivity of the molecules increases as ΔE decreases, because the energy needed to remove an electron from the last occupied molecular orbital will be less [58]. Thus, smaller the energy gap
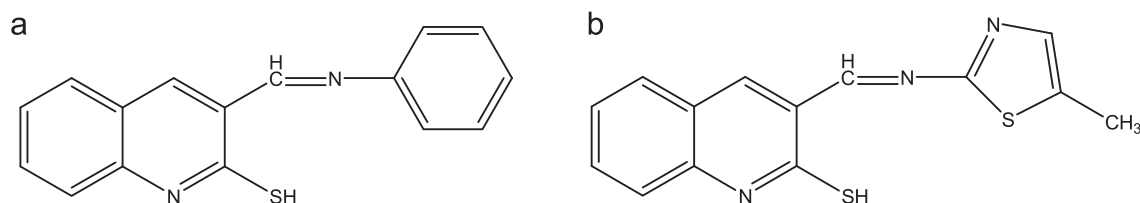

Fig. 1. Chemical structure of the studied corrosion inhibitors: (a) 3-((phenylimino)methyl)quinoline-2-thiol (PMQ) and (b) 3-((5-methylthiazol-2-ylimino)methyl)quinoline-2-thiol (MMQT).
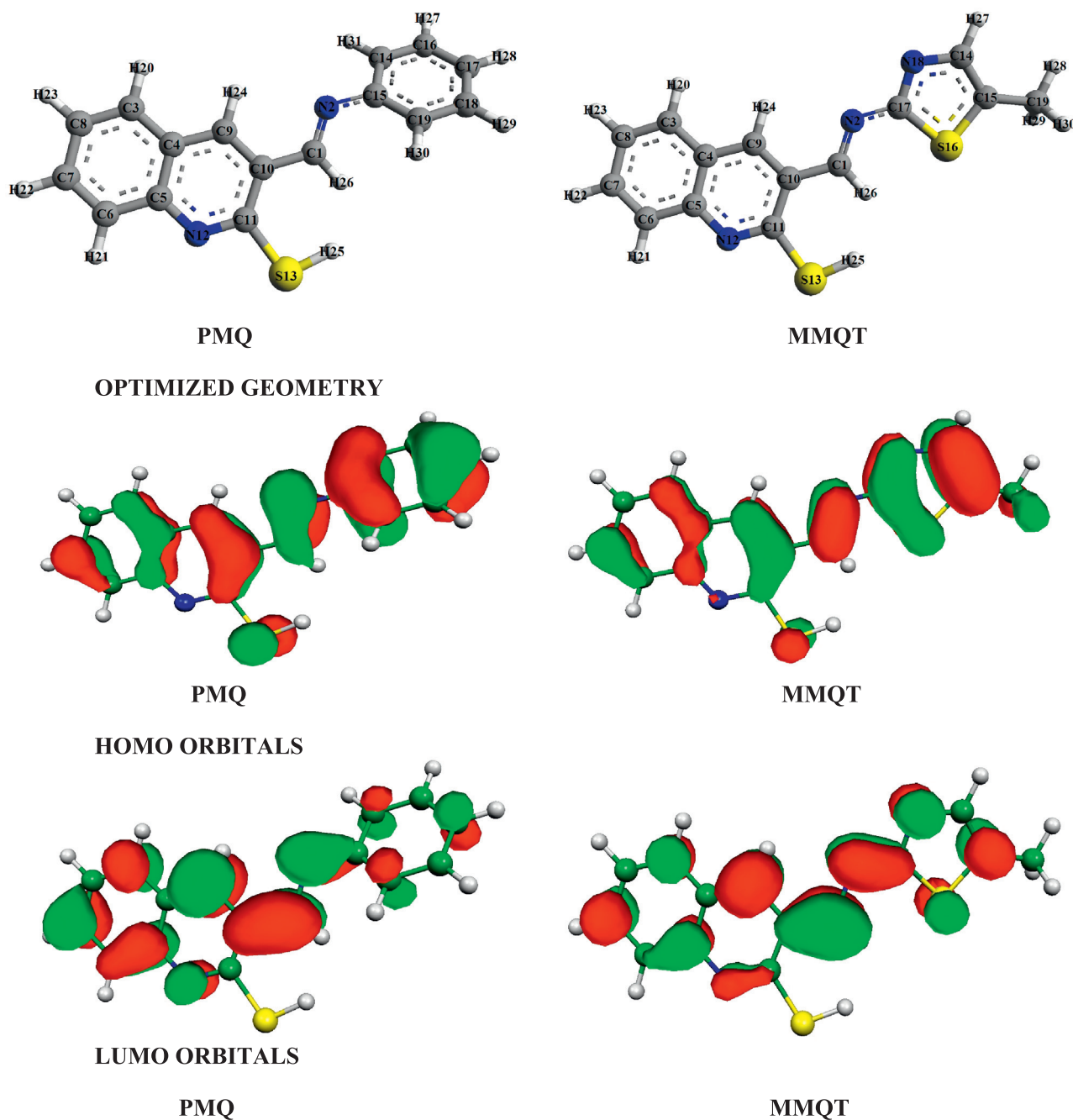
PMQ   **MMQT**

OPTIMIZED GEOMETRY

PMQ   **MMQT**

HOMO ORBITALS

LUMO ORBITALS

PMQ   **MMQT**

Fig. 2. The optimized geometry: HOMO and LUMO orbitals of PMQ and MMQT at the B3LYP/SV(P), SV/J level of basic set for neutral species in aqueous phase.

(ΔE) more it will be polarizable and better will be the electrons transport. It is observed from Table 2, MMQT has smaller energy gap (ΔE) as compared to PMQ. Dipolemoment (μ) of a molecule is related to the polarity of the polar covalent bond. It is defined as the product of charge (in magnitude on respective atoms) and the distance between the two concerned atoms. A literature survey reveals that there are several irregularities in the relationship between dipolemoment and the experimentally obtained inhibition efficiency [59–62]. In this present work, it can be seen (*vide* Table 2) that dipolemoment decreases in the trend similar to that of E_{HOMO}, E_{LUMO} and ΔE. A comparison of present theoretical outcomes and previously obtained experimental results supports

Table 2
Calculated quantum chemical parameters of the studied inhibitors.

Inhibitors	E_{HOMO} (eV)	E_{LUMO} (eV)	ΔE (eV)	μ(Debye)	$I=-E_{HOMO}$	$A=-E_{LUMO}$	χ	η	S	ΔN	Inhibition efficiency[a]
PMQ	−6.2428	−2.3723	3.8705	2.8489	6.2428	2.3723	4.3075	1.9352	0.5167	0.6956	96.00
MMQT	−6.1707	−2.7461	3.4246	2.4124	6.1707	2.7461	4.4584	1.7123	0.5840	0.7421	99.11

[a] Values obtained from Ref. [35].

that MMQT has greater potentiality compared to PMQ to get adsorbed on the mild steel surface.

The ionization potential (I) and electron affinity (A) of the inhibitors can be calculated by the application of Koopmans' theorem [63]. According to this theorem, the ionization potential is related to the HOMO energy whereas electron affinity is related to the LUMO energy of the molecules, respectively. Formal authentication of this theorem is not presented within DFT; however, its validity is accepted from long before. The ionization potential and electron affinity values are used to obtain the elctronegativity (χ) and global hardness (η) of molecules of interest. These parameters are related to ionization potential and electron affinity by the following formula:

$$\chi = \frac{I + A}{2} \tag{6}$$

The global hardness η defined as

$$\eta = \frac{I - A}{2} \tag{7}$$

A and I are related to E_{HOMO} and E_{LUMO} as follows:

$$A = -E_{LUMO} \tag{8}$$

$$I = -E_{HOMO} \tag{9}$$

The fraction of electron transferred from the inhibitor molecule to the metallic surface (ΔN) is calculated by the Pearson method [64]. The difference in electronegativities between the two systems (metallic surface and inhibitor molecule) is responsible for the corresponding electron transfer. Electron flow will happen from the molecule with low electronegativity towards that of higher value until the chemical potentials are same. The fraction of electron transfers to the metallic surface is calculated as follows:

$$\Delta N = \frac{\chi_{Fe} - \chi_{inh}}{2(\eta_{Fe} + \eta_{inh})} \tag{10}$$

For Fe, the theoretical value of χ_{Fe} and η_{Fe} are 7 eVand 0 eV, respectively [64,65]. Electron transfer will occur from molecule to metal surface if $\Delta N > 0$ and vice versa if $\Delta N < 0$ [25,26,66]. According to Elnga et al. [29], inhibition efficiency increases with increasing electron-donating ability of the molecule at the metal surface if $\Delta N < 3.6$. Table 2 shows that both the values of ΔN are positive and less than 3.6, indicating that the molecule donates its electron to the Fe surface by the formation of a coordinate bond. It is also noticed that only slight differences in the fraction of electron transfer are observed for the two inhibitor molecules when they interact with the so-called Fe surface. This suggests a similar electron donating capability for the two studied inhibitor molecules. Combining the results obtained from frontier molecular orbitals and frontier orbital energies, we may conclude that the difference in inhibition efficiency is mainly related to the different capabilities of the molecules to accept electrons from the metal surface (*vide Supra*).

Global softness (S) is also an important parameter (reciprocal of hardness, $1/\eta$) concerning the adsorption of inhibitor molecule on the metal surface. In corrosion inhibition chemistry, the inhibitors are considered as soft base and the metals as soft acid [67]. Therefore, soft–soft interaction is the most predominant factor for the adsorption of inhibitor molecules. It can be seen (*vide* Table 2) that the calculated values of softness follow the order MMQT > PMQ, which once again supports the better adsorption power of MMQT on the metal surface.

Table 3
Calculated Fukui functions for the two inhibitor molecules.

Inhibitors	Atom	f_k^+	f_k^-
PMQ	C (1)	0.081	0.024
	N (2)	0.072	0.033
	C (3)	0.046	0.036
	C (4)	0.026	0.029
	C (5)	0.037	0.029
	C (6)	0.035	0.043
	C (7)	0.057	0.032
	C (8)	0.031	0.051
	C (9)	0.087	0.031
	C (10)	0.047	0.025
	C (11)	0.019	0.032
	N (12)	0.040	0.057
	S (13)	0.061	0.244
	C (14)	0.026	0.022
	C (15)	0.016	0.023
	C (16)	0.018	0.019
	C (17)	0.033	0.034
	C (18)	0.019	0.018
	C (19)	0.026	0.024
MMQT	C (1)	0.091	0.035
	N (2)	0.065	0.031
	C (3)	0.036	0.030
	C (4)	0.021	0.024
	C (5)	0.032	0.025
	C (6)	0.026	0.033
	C (7)	0.047	0.031
	C (8)	0.025	0.037
	C (9)	0.071	0.032
	C (10)	0.035	0.026
	C (11)	0.017	0.026
	N (12)	0.030	0.041
	S (13)	0.056	0.170
	C (14)	0.031	0.057
	C (15)	0.040	0.053
	S (16)	0.091	0.073
	C (17)	0.029	0.039
	N (18)	0.056	0.038
	C (19)	0.012	0.015

3.2. Active sites

Inhibitor molecules can bind with metal surface by electron transfer (donating or accepting). Therefore, in an inhibitor it is essential to examine the active sites of interaction. To investigate the active sites of an inhibitor, mostly there are three controlling factors which have to be considered: (i) neutral atomic charge, (ii) distribution of frontier molecular orbital and (iii) Fukui indices. Fukui indices are used to analyze the local reactivity of the studied inhibitors [47]. It provides entire information about the reactive centers and indicates their chemical reactivity for nucleophilic and electrophilic nature[68]. The nucleophilic and electrophilic attacks are controlled by the maximum threshold values of f_k^+ and f_k^-. The preferred sites for nucleophilic attacks are the atoms or the regions where the value of f_k^+ is the highest; similarly, electrophilic attacks are preferred where the value of f_k^- is the largest. Calculated Fukui indices of the two studied molecules are presented in Table 3. It can be seen (*vide* Table 3) that for PMQ molecules C(1), N(2), C(7), C(9) and S(13), atoms are responsible for nucleophilic attack, as those pose the highest value of f_k^+, 0.081 for C(1), 0.072 for N(2), 0.057 for C(7), 0.087 for C(9) and 0.061 for S(13), respectively. On the contrary, C(8), N(12) of quinoline ring along with S(13) of its adjacent side arm are the most susceptible sites for electrophilic attack as they present the highest value of f_k^-, *e.g.*, 0.051 for C(8), 0.057 for N(12) and 0.244 for S(13). It can be concluded from these results that azomethine linkage and quinoline ring are the most responsible sites for nucleophilic attack, whereas quinoline ring is responsible for electrophilic attack.

Benzene ring of the PMQ when is replaced by 5-methylthiazole, producing MMQT, the distribution of active sites is quite different. In MMQT, the highest values of f_k^+ are located on the C(1), N(2), C(9), S(13), S(16) and N(18) atoms, which implies that mostly all segments of the MMQT molecule are responsible for the nucleophilic attack, whereas electrophilic attack is mainly controlled by the thiazole ring and the –SH side arm of the quinoline ring; as C, N and S atoms of that unit has the highest value of f_k^-.

Based on the above discussion, it can be concluded that PMQ and MMQT have many active sites for adsorption on the mild steel surface. These results are also in good accordance with experimentally obtained inhibition efficiency.

3.3. Molecular dynamics simulation

In recent times, MD simulation has emerged as a modern tool to investigate the interaction between the inhibitors with the metal surface. Musa et al. have employed MD simulation to study the corrosion behavior of phthalazine derivatives on a mild steel surface [69]. Xia et al. have studied the inhibition performance of several substituted imidazoline derivatives by applying molecular dynamics and it was concluded that all these molecules adsorbed on the Fe surface through the imidazoline ring and its heteroatoms [31]. For a better insightfulness into the adsorption behavior of PMQ and MMQT, MD simulations are performed to analyze the interaction of the two studied Schiff base inhibitors on the Fe (1 1 0) surface.

The binding strength of the two Schiff base type inhibitors on the Fe surface is calculated by MD simulations, which can be determined by a clear relationship between the binding energies of these aforementioned inhibitors (determined theoretically) along with experimentally obtained inhibition efficiencies. In order to get this, first of all geometry optimization of the two studied inhibitors is carried out employing a 'smart' algorithm which started with the steepest descent method then followed the conjugate gradient method and finally ended with the Newton's method as described in [44]. During geometry optimization, atomic coordinates are adjusted based on COMPASS forcefield [51] until and unless the total energy of the individual structure reaches the minimum energy, afterwards inhibitors are placed on the Fe (1 1 0) surface to find out the most suitable and adorable adsorption configuration. After the system reaches an equilibrium, the values of E_{total}, $E_{surface}$ and $E_{inhibitor}$ are calculated by single point energy calculation, then interaction energy ($E_{interaction}$)

between Fe (1 1 0) surface and corresponding inhibitors can be evaluated following Eq. (4). The system reaches equilibrium only when the temperature and energy reach a balance. Temperature and energy fluctuation curves are shown (*vide* Figs. 3 and 4) for the interaction between PMQ and MMQT on the Fe (1 1 0) surface. It is well understood (*vide* Figs. 3 and 4) that in the middle of the modeling process the system has a tendency to be in equilibrium. The close contacts of the concerned Fe surface and inhibitors of interest along with the best adsorption configuration of the inhibitors on the Fe (1 1 0) surface are depicted in Fig. 5. From Fig. 5, it is noticed that the two inhibitor molecules are adsorbed on the Fe (1 1 0) plane with almost parallel or flat disposition, it confirms that strong interactions happen between the inhibitor molecule and the Fe atoms. The flat orientation of the inhibitor molecule with respect to the Fe surface will definitely provide larger blocking area for the adsorption and thus higher inhibition efficiency is expected and is also observed accordingly.

The calculated values of interaction energies of the adsorption systems are –150.764 and –155.367 kcal mol^{-1} for PMQ and MMQT, respectively. The higher negative values of interaction energy can be attributed to the strong adsorption of inhibitor molecules on the Fe surface [70]. Moreover, the adsorption ability can also be measured from the binding energy of the molecule with the Fe surface. Higher the value of binding energy, more stable will be the adsorption of the molecule on the Fe surface. It can be seen (Table 4) that the order of binding energy is as follows: MMQT > PMQ. Thus, MMQT has better adsorption ability on the Fe surface than PMQ. These results are in good agreement with the previous results obtained from wet chemical experimental work [35] as well as from quantum chemical calculations of the present work.

3.4. Comparison of theoretical analysis with experimental outcomes

Corrosion inhibition for mild steel in 1 M HCl media using two marcaptoquinoline Schiff base inhibitors is investigated by weight loss, potentiodynamic polarization and electrochemical impedance spectroscopic-like experimental studies and their order of inhibition efficiency is as follows: PMQ < MMQT [35]. In this present work, a vivid theoretical experimentation and a finer comparison with the wet chemical experimental outcomes for these two inhibitors are in good accordance. First of all, according to quantum chemical outcomes, both the inhibitors have multiple active centers, where the adsorption on the metallic surface could
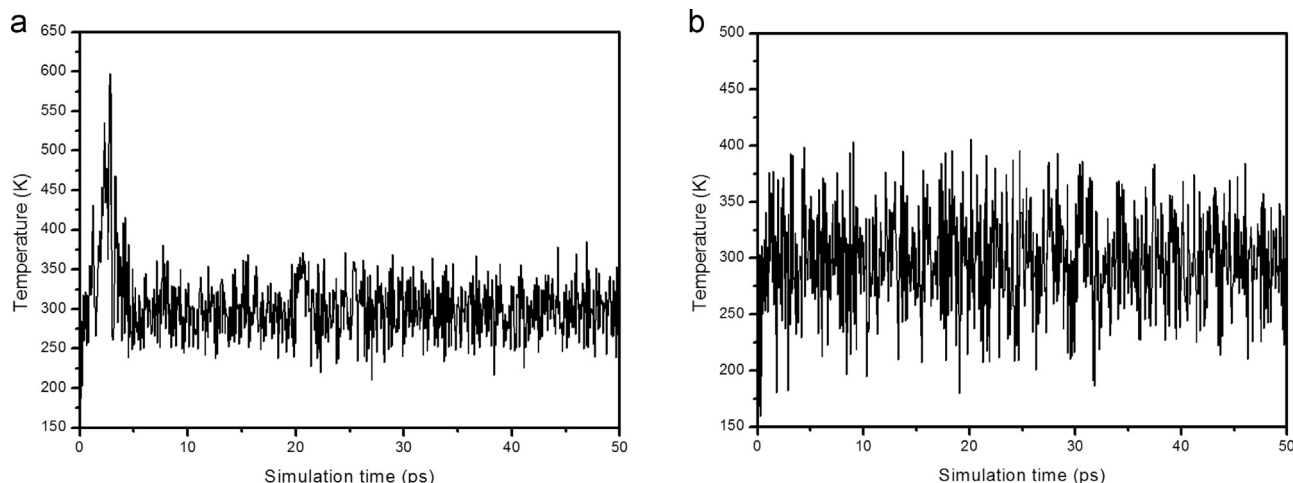

Fig. 3. Temperature equilibrium curve obtained from MD simulation for (a) PMQ and (b) MMQT.
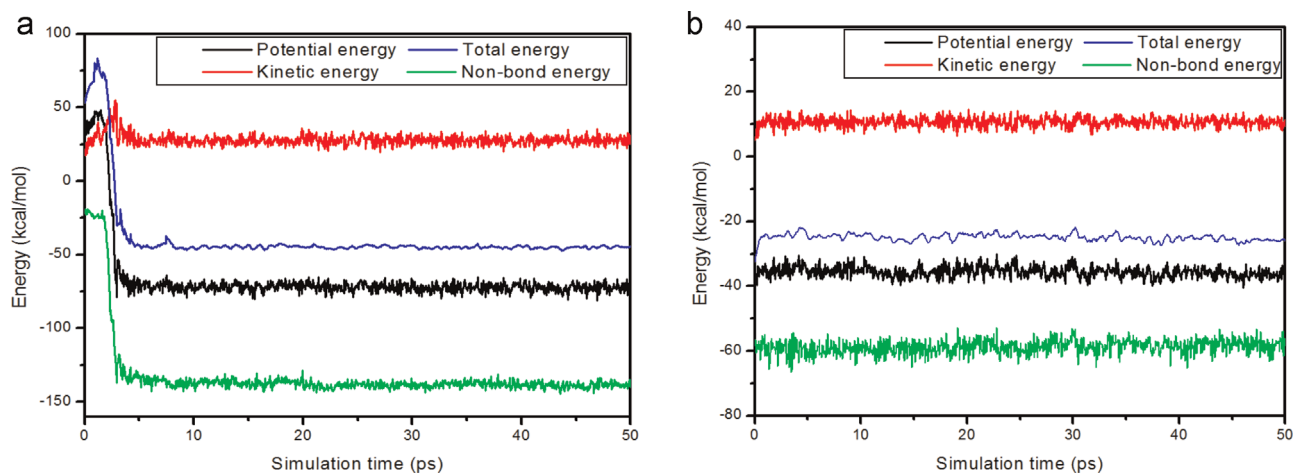
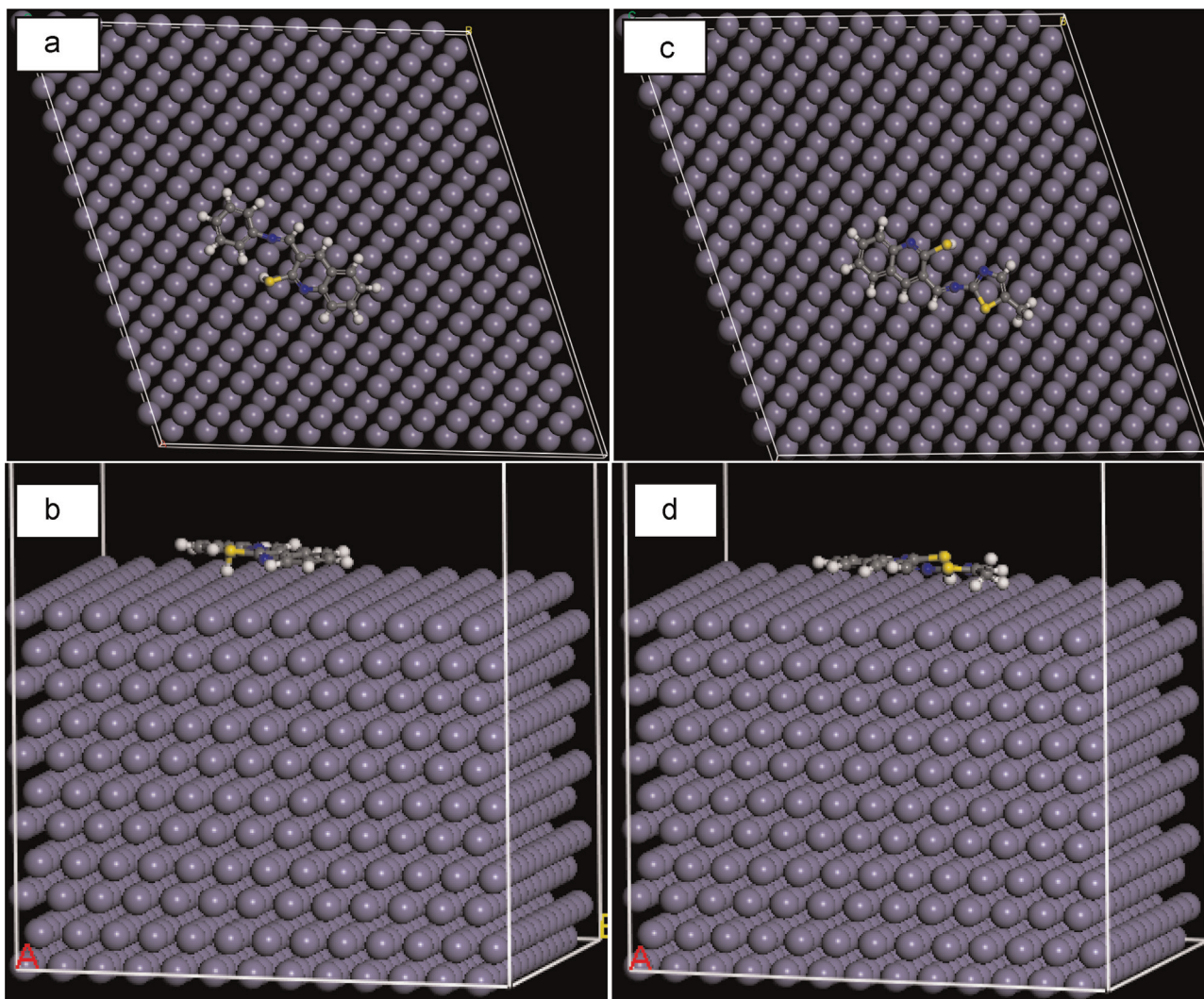**Fig. 4.** Energy fluctuation curves obtained from MD simulation for (a) PMQ and (b) MMQT.

Fig. 5. Equilibrium adsorption configurations of inhibitors PMQ (a and b) and MMQT (c and d) on Fe (1 1 0) surface obtained by MD simulations. Top: top view, bottom: side view.

be possible. All the theoretically obtained quantum chemical parameters indicate that the order of inhibition efficiency is MMQT > PMQ, which agrees well with the experimental results. Furthermore, MD simulation shows that a flat or parallel disposition of adsorption of inhibitors on the Fe surface occurs and it also follows the binding energy order of MMQT > PMQ, which is again well in agreement with the experimental findings. This present study strengthens the fact that for a better perspective and

Table 4
Output obtained from MD simulation for adsorption of inhibitors on Fe (1 1 0) surface.

Systems	$E_{interaction}$ (kcal/mol)	$E_{binding}$ (kcal/mol)
Fe+PMQ	− 150.764	150.764
Fe+MMQT	− 155.367	155.367

for a futuristic quick prediction, this combined methodology will be very fruitful towards prediction of inhibition phenomenon of a series of unknown inhibitors.

4. Conclusion

A combined classical and quantum chemical approach is performed to correlate the inhibition performance of two experimentally studied mercapto-quinoline Schiff base inhibitors. Examination of reactivity of the inhibitors from molecular to atomistic level offers the realistic insightfulness and supports in favor of their wet chemical outcomes. The following insightful conclusions could be depicted from this present study:

(i) There is a steric effect of PMQ compared to MMQT, which causes a deviation from planar structure. DFT(ORCA) simulation shows that spatial distributions of MMQT are almost in a horizontal orientation in aqueous solution whereas that for PMQ shows a tilted orientation, responsible for less inhibition effect.
(ii) Active sites of the inhibitor molecules for adsorption on the metallic surface are thoroughly investigated by DFT (Dmol^3). Fukui indices describe in detail the electrophilic as well as nucleophilic attacking center where a corresponding electrophilic and nucleophilic interaction may occur.
(iii) The binding energy values of the two inhibitor compounds with the Fe (1 1 0) surface obey the order MMQT > PMQ, in accordance with the experimental inhibition efficiency.

In summary, all these studies are in good agreement with the results obtained from three different domains starting from quantum chemical calculation (based on quantum chemistry) to molecular dynamics simulation (based on classical physics) and finally to previously explored wet chemical experimentation. From all these successful correlations, it can be concluded that DFT along with MD can be successfully implemented for rational designing of several promising inhibitor molecules without performing even a single expensive wet chemical experimental study.

References

[1] S.A. AbdEl-Maksoud, A.S. Fouda, Mater. Chem. Phys. 93 (2005) 84–90.
[2] H. Keles, M. Keles, I. Dehri, O. Serindag, Mater. Chem. Phys. 112 (2008) 173–179.
[3] H. Wang, H. Fan, J. Zheng, Mater. Chem. Phys. 77 (2003) 655–661.
[4] M. Abdallah, Corros. Sci. 45 (2003) 2705–2716.
[5] M. Lagrenee, B. Mernari, M. Bouanis, M. Traisnel, F. Bentiss, Corros. Sci. 44 (2002) 573–588.
[6] F. Bentiss, M. Lagrenee, M. Trainsel, J.C. Hornez, Corros. Sci. 41 (1999) 789–803.
[7] H. Ashassi-Sorkhabi, N. Ghalebsaz-Jeddi, F. Hashemzadeh, H. Jahani, Electrochim. Acta 51 (2006) 3848–3854.
[8] H. Ju, Z.P. Kai, Y. Li, Corros. Sci. 50 (2008) 865–871.
[9] M. Elayyachy, B. Hammouti, A. El Idrissi, Appl. Surf. Sci. 249 (2005) 176–182.
[10] E.E. Foad El Sherbini, Mater. Chem. Phys. 60 (1999) 286–290.
[11] M. Ajmal, A.S. Mideen, M.A. Quaraishi, Corros. Sci. 36 (1994) 79–84.
[12] R. Hasanov, M. Sadıkoglu, S. Bilgic, Appl. Surf. Sci. 253 (2007) 3913–3921.
[13] S. Deng, X. Li, H. Fu, Corros. Sci. 53 (2011) 822–828.
[14] F. Bentiss, M. Traisnel, L. Gengembre, M. Lagrenee, Appl. Surf. Sci. 152 (1999) 237–249.
[15] M.G.V. Satyanarayana, V. Himabindu, Y. Kalpana, M.R. Kumar, K. Kumar, J. Mol. Struc. (Theochem) 912 (2009) 113–116.
[16] T.H. Muster, A.E. Hughes, S.A. Furman, T. Harvey, N. Sherman, S. Hardin, P. Corrigan, D. Lau, F.H. Scholes, P.A. White, M. Glenn, J. Mardel, S.J. Garcia, J.M. C. Mol, Electrochim. Acta 54 (2009) 3402–3411.
[17] T. Ghailane, R.A. Balkhmima, R. Ghailane, A. Souizi, R. Touir, M. Ebn Touhami, K. Marakchi, N. Komiha, Corros. Sci. 76 (2013) 317–324.
[18] T. Arslan, F. Kandemirli, E.E. Ebenso, I. Love, H. Alemu, Corros. Sci. 51 (2009) 35–47.
[19] B.D. Mert, M.E. Mert, G. Kardas, B. Yazıcı, Corros. Sci. 53 (2011) 4265–4272.
[20] I.B. Obot, N.O. Obi-Egbedi, Corros. Sci. 52 (2010) 657–660.
[21] K.R. Ansari, M.A. Quraishi, A. Singh, Corros. Sci. 79 (2014) 5–15.
[22] A. Ehsani, M.G. Mahjani, R. Moshrefi, H. Mostaanzadeha, J.S. Shayehb, RSC Adv. 4 (2014) 20031–20037.
[23] S. John, M. Kuruvilla, A. Joseph, RSC Adv. 3 (2013) 8929–8938.
[24] A. Kokalj, S. Peljhan, M. Finšgar, I. Milošev, J. Am. Chem. Soc. 132 (2010) 16657–16668.
[25] A. Kokalj, Electrochim. Acta. 56 (2010) 745–755.
[26] N. Kovačević, A. Kokalj, Corros. Sci. 53 (2011) 909–921.
[27] E.E. Ebenso, M.M. Kabanda, L.C. Murulana, A.K. Singh, S.K. Shukla, Ind. Eng. Chem. Res. 51 (2012) 12940–12958.
[28] Sudheer, M.A. Quraishi, Corros. Sci. 70 (2013) 161–169.
[29] M.K. Awad, M.R. Mustafa, M.M.A. Elnga, J. Mol. Struct.(Theochem) 959 (2010) 66–74.
[30] Y. Tang, X. Yang, W. Yang, R. Wan, Y. Chen, X. Yin, Corros. Sci. 52 (2010) 1801–1808.
[31] S. Xia, M. Qiu, L. Yu, F. Liu, H. Zhao, Corros. Sci. 50 (2008) 2021–2029.
[32] B. Xu, Y. Liu, X. Yin, W. Yang, Y. Chen, Corros. Sci. 74 (2013) 206–213.
[33] S.K. Saha, P. Ghosh, A.R. Chowdhury, P. Samanta, N.C. Murmu, A.K. Lohar, P. Banerjee, Can. Chem. Trans. 2 (2014) 381–402.
[34] S.K. Saha, A. Hens, A.R. Chowdhury, A.K. Lohar, N.C. Murmu, P. Banerjee, Can. Chem. Trans. 2 (2014) 489–503.
[35] B.M. Mistry, S. Jauhari, Chem. Eng.Commun. 201 (2014) 961–981.
[36] K.F. Khaled, Electrochim. Acta 55 (2010) 6523–6532.
[37] F. Neese, An Ab initio, DFT and Semiempirical SCF-MO Package, version 2.9, Max Planck Institute for Bioinorganic Chemistry, Mulheim an der Ruhr, Germany, 2012.
[38] D.A. Becke, J. Chem. Phys. 84 (1986) 4524–4529.
[39] D.A. Becke, J. Chem. Phys. 98 (1993) 5648–5652.
[40] C. Lee, W. Yang, G.R. Parr, Phys. Rev. B 37 (1988) 785–789.
[41] P. Banerjee, A. Company, T. Weyhermuller, E. Bill, C.R. Hess, Inorg. Chem. 48 (2009) 2944–2955.
[42] A. Schafer, C. Huber, R. Ahlrichs, J. Chem. Phys. 100 (1994) 5829–5835.
[43] A. Schafer, H. Horn, R. Ahlrichs, J. Chem. Phys. 97 (1992) 2571–2577.
[44] Materials Studio 6.1 Manual, Accelrys, Inc., San Diego, CA, 2007.
[45] Z. Cao, Y. Tang, H. Cang, J. Xu, G. Lu, W. Jing, Corros. Sci. 83 (2014) 292–298.
[46] J.A. Ciezak, S.F. Trevino, J. Phys. Chem. A 110 (2006) 5149–5155.
[47] R.G. Parr, W. Yang, J. Am.Chem. Soc. 106 (1984) 4049–4050.
[48] F.D. Proft, J.M.L. Martin, P. Geerlings, Chem. Phys. Lett. 256 (1996) 400–408.
[49] R.R. Contreras, P. Fuentealba, M. Galvan, P. Perez, Chem. Phys. Lett. 304 (1999) 405–413.
[50] F.L. Hirshfeld, Theor. Chem. Acc. 44 (1977) 129–138.
[51] H. Sun, J. Phys. Chem. B 102 (1998) 7338–7364.
[52] N.A. Al-Mobarak, K.F. Khaled, M.N.H. Hamed, K.M. Abdel-Azim, N. S. Abdelshafi, Arab. J. Chem 3 (2010) 233–242.
[53] A.F. Brigas, W. Clegg, C.J. Dillon, C.F.C. Fonseca, R.A.W. Johnstone, J. Chem. Soc. Perkin Trans. 2 (2001) 1315–1324.
[54] H.G. Raubenheimer, E.K. Marais, S. Cronje, C. Esterhuysen, G.J. Kruger, J. Chem. Soc. Dalton. Trans. (2000) 3016–3021.
[55] T. Eicher, S. Hauptmann, A. Speicher, The Chemistry of Heterocycles: Structures, Reactions, Synthesis, and Applications, Wiley, 2012.
[56] G. Gece, Corros. Sci. 50 (2008) 2981–2992.
[57] R.G. Pearson, J. Chem. Educ. 64 (1987) 561–567.
[58] K.F. Khaled, Electrochim. Acta 48 (2003) 2493–2503.
[59] M. Sahin, G. Gece, F. Karci, S. Bilgic, J. Appl. Electrochem. 38 (2008) 809–815.
[60] M.A. Quraishi, R. Sardar, J. Appl. Electrochem. 33 (2003) 1163–1168.
[61] K.F. Khaled, N.K. Babic-Samardzija, N. Hackerman, Electrochim. Acta 50 (2005) 2515–2520.
[62] G. Bereket, E. Hur, C. Ogretir, J. Mol. Struct. (Theochem) 578 (2002) 79–88.
[63] I. Lukovits, E. Kalman, F. Zucchi, Corrosion 57 (2001) 3–8.

[64] S. Martinez, Mater. Chem. Phys. 77 (2002) 97–102.
[65] M.J.S. Dewar, W. Thiel, J. Am. Chem. Soc. 99 (1977) 4899–4907.
[66] N. Kovačević, A. Kokalj, J.Phys. Chem. C 115 (2011) 24189–24197.
[67] I.B. Obot, Z.M. Gasem, Corros. Sci. 83 (2014) 359–366.
[68] M.A. Hegazy, A.M. Badawi, S.S. Abd El Rehim, W.M. Kamel, Corros. Sci. 69 (2013) 110–122.

[69] A.Y. Musa, R.T.T. Jalgham, A.B. Mohamad, Corros. Sci. 56 (2012) 176–183.
[70] A.Y. Musa, A.A.H. Kadhum, A.B. Mohamad, M.S. Takriff, Corros. Sci. 52 (2010) 3331–3340.